NEUTRON ENRICHMENT AT MIDRAPIDITY IN ^{58}Ni + ^{58}Ni AT 52 MeV/u

D. Thériault[1], the INDRA Collaboration, A. Vallée[1], L. Gingras[1], Y. Larochelle[1], R. Roy[1], A. April[1], L. Beaulieu[1], F. Grenier[1], F. Lemieux[1], J. Moisan[1], M. Samri[1], C. St-Pierre[1], S. Turbide[1], S.J. Yennello[2], E. Martin[2], E. Winchester[2],
[1] *Laboratoire de Physique Nucléaire,Département de Physique, Université Laval, Québec, Canada G1K 7P4. and*
[2] *Cyclotron Institute, Texas A&M University, College Station, Texas, U.S.A.*

Abstract

By combining data from a charged particle ^{58}Ni+^{58}Ni experiment at 52 MeV/u with an ^{36}Ar+^{58}Ni experiment at 50 MeV/u for which free neutrons have been detected, an increase in the neutron to proton ratio of the whole nuclear material at midrapidity has been experimentally observed in the reaction ^{58}Ni+^{58}Ni at 52 MeV/u. The neutron to proton ratio is measured above the initial neutron to proton ratio of the system. Neutron to proton ratio of the quasi-projectile emission is analyzed for the same reactions and is seen to decrease below the ratio of the initial system.

1. INTRODUCTION

In recent years, a source of emission between the target rapidity and that of the projectile has been evidenced and characterized in heavy ions collisions at intermediate energies [1–12] and theoretically studied [13, 14]. Interestingly, light particles and fragments emitted by that midrapidity source (MRS) exhibit a neutron enrichment compared to those from the quasiprojectile (QP) or the quasitarget (QT) [15–18]. This fact could be due to the abundance of symmetric clusters [19] or Coulomb effects [19, 20] and does not imply a neutron enrichment of the total nuclear matter at midrapidity. Therefore, the analysis of the whole MRS material is of interest. To explain the neutron abundance of a supposed low-density MRS, a density dependence in the symmetry energy term of the nuclear equation of state has been suggested [21–23]. In the present article, we report on an experimental evaluation of the MRS and QP N/Z ratios as a function of the centrality of the collision. The ^{58}Ni+^{58}Ni reaction is studied at 52 MeV/u and the free-neutron multiplicities are extracted from the analysis of the ^{36}Ar+^{58}Ni reaction at 50 MeV/u.

2. EXPERIMENTAL APPARATUS

The charged particle experiment has been performed at the GANIL facility using a ^{58}Ni beam accelerated to 52 MeV/u bombarding a self-supporting 0.179 mg/cm^2 ^{58}Ni target. The charged reaction products were detected with the INDRA detector, which consists of 336 detection modules mounted on 17 rings covering polar angles from 2^0 to 176^0. The first inner ring is made of fast-slow plastic phoswich detectors. Rings 2 to 9 consist of a triple telescope, with an ionization chamber, Si detector and CsI(Tl) scintillator. Rings 10 to 17 consist of an ionization chamber and a CsI scintillator. Elements were identified by their charge up to Z=28 and isotopic resolution was achieved up to Z=4. A complete description of the INDRA detector is given in Ref.[24].

For the neutron detection experiment at the Cyclotron Institute of Texas A&M University, a ^{36}Ar beam has been accelerated to 50 MeV/u on a 5.0 mg/cm^2 ^{58}Ni target. The charged reaction products were collected with the HERACLES array. The first five rings of the array are made of fast-slow plastic phoswich detectors located between 1.3^0 and 24^0. Two other rings, covering angles from 24^0 to 46^0, are made of CsI(Tl) scintillators. Neutrons were detected with eight Bicron BC-501 liquid scintillator units located outside the reaction chamber at polar angles between 60^0 and 150^0. Neutron energies were determined by time-of-flight measurements and spectra were corrected for background emission using a shadow bar technique. An experimental response function for the BC-501 detector [25] was used for efficiency corrections. Attenuation

in the chamber wall was taken into account.

3. ANALYSIS

3.1. *Source and event selection in ^{58}Ni+^{58}Ni*

In the present analysis, only isotopically well identified elements ranging from Z=1 to Z=4 were used in ring 2 to 12 of the INDRA multidetector (3^0 to 88^0). Events containing non isotopically-resolved elements from Z=1 to Z=4 in those forward rings were rejected. The elements with $Z \geq 5$ were accepted in ring 1 to ring 9 of the INDRA multidetector (2^0 to 45^0). The mass assumed for those heavier elements is based on the evaporation attractor line of Charity [26], or on the initial N/Z of the system for Z≥25. The MRS is not affected by those last analysis conditions, since it is composed almost exclusively of Z=1-4 elements. The heaviest fragment in the forward direction is taken as the QP evaporation residue. Events selection criteria for the residue are: parallel velocity greater than 70% of the beam velocity and charge (Z_{res}) greater or equal to 10. This selection of peripheral and mid-peripheral events is made to avoid contamination of the QP forward hemisphere (particles with parallel velocities greater than that of the residue) by other sources or non-statistical emission, and to apply the QP reconstruction procedure in its optimal range of efficiency. Also, only events with a total detected charge of 28 or more in the INDRA multidetector and $\Sigma P_{||} \geq 66\% P_{||initial}$ were analysed.

Since the goal of the present analysis is to evaluate the MRS and QP N/Z ratios in the ^{58}Ni+^{58}Ni reaction at 52 MeV/u, it is important to disentangle the QP emitted material from the nuclear material emitted by the MRS in this reaction. Attribution of bound particles ($A \geq 2$) to the QP source is done via a weighting method. MRS emission is selected as non-QP particles with a parallel (beam direction) velocity higher than a specified velocity cut to isolate them from QT emission. The free protons and neutrons, because of a significant overlap in source emission were treated differently. Multisource analysis for free nucleons is presented below.

The QP source reconstruction procedure, applied to the ^{58}Ni+ ^{58}Ni reaction, relies on three hypotheses [27]: 1)the heaviest fragment selected as the QP evaporation residue has a velocity that is approximatively the QP velocity, 2)the QP emission is isotropic in its reference frame and 3)all the particles with a parallel velocity greater than that of the residue (forward distribution) were emitted from the QP. V_{rel}(norm of the relative velocity between a particle and the residue) spectra are made for each pair of isotope and Z_{res}. Using V_{rel} spectra, probability tables for the attribution of an isotope to the QP are built. Attribution probability is fixed at unity for forward emitted particles while the probability for backward particles (parallel velocity less than that of the QP residue) is obtained by dividing the forward V_{rel} distribution by the backward distribution. The probability tables are applied on an event-by-event basis to reconstruct the QP, each particle in the backward distribution having a probability to be attributed to the QP according to its specific value of V_{rel} and Z_{res}. More details about the reconstruction method and its efficiency are given in Ref. [7, 9, 27]. Backward emitted particles that were not attributed to the QP were attributed to the MRS if their parallel velocity was greater than 2 cm/ns in the reference frame of the QT which is moving at velocities determined in the proton multisource analysis. That limit, 2 cm/ns, is a confidence value established from the QP parallel velocity distributions in the forward distribution, to build a MRS sample with little pollution from the QT.

To include free protons in the analysis, average proton multiplicities are extracted for four classes of events sorted according to Z_{res}(^{58}Ni):$10-13$, $14-18$, $19-23$ and $24-28$, characterizing the centrality of the reaction. Multiplicities are obtained via moving source analysis of energy spectra at 16 angles from the INDRA detector. The energy spectra are fitted simultaneously with the summation of three sources, QP, QT and MRS, each being characterized by its temperature T , its velocity V_s, its Coulomb barrier B_c and its proton multiplicity N. The proton energy (E) distribution is fitted under the assumption of surface emission for the QT and QP sources and volume emission for the MRS by [11, 28–30]:

$$(\frac{d^2\sigma}{d\Omega dE})_{sur} = \frac{N}{4\pi T^2}(E - B_c)\exp[-(E - B_c)/T] \quad (1)$$

and

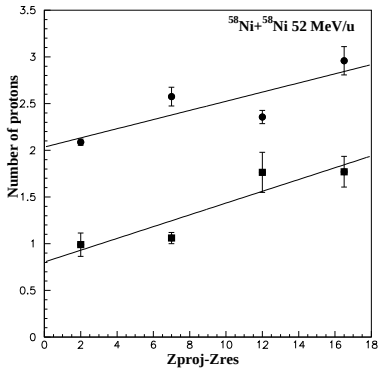

FIG. 1: Linearized proton multiplicities for ^{58}Ni+^{58}Ni at 52 MeV/u as a function of the projectile charge minus the QP residue charge. QP (dots) and MRS (squares) multiplicities are illustrated.

$$(\frac{d^2\sigma}{d\Omega dE})_{vol} = \frac{N}{2(\pi T)^{3/2}}\sqrt{(E-B_c)}\exp[-(E-B_c)/T] \quad (2)$$

respectively. The transformation to the laboratory frame takes into account the angle θ of the detector and the velocity V_S of the emitting source [28–30]. Overall, proton multiplicities increase smoothly with centrality. Fig. 1 shows the extracted proton multiplicities as a function of Z_{proj}(^{58}Ni)-Z_{res}(^{58}Ni).

3.2. *Free neutron evaluation in ^{36}Ar+^{58}Ni*

The multisource fit for free neutrons is done on spectra from the ^{36}Ar+^{58}Ni experiment. The events are sorted into four classes according to Z_{res}(^{36}Ar):$4-6$, $7-9$, $10-14$ and $15-20$. Since forward angles were not covered by the neutron detectors, energy spectra are fitted with the summation of two moving sources, QT and MRS. The neutron energy (E) distribution is fitted under the assumption of surface emission for the QT source and volume emission for the MRS, using eq.(1) and eq.(2) without Coulomb barriers. Fig. 2 shows fits of the neutron energy spectra for one class. Fig. 3 presents the corresponding free neutron multiplicities as a function of the projectile charge minus the QP residue charge. The deduced multiplicities for the MRS increase steadily with centrality and reache a value of 2.3 while QT multiplicities are stabilizing just above

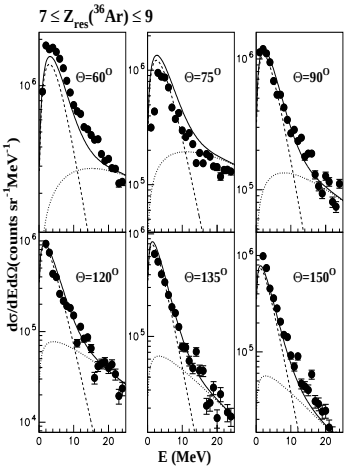

FIG. 2: Neutron energy spectra corrected for background emission and efficiency of six detectors for one centrality class of the ^{36}Ar+^{58}Ni reaction at 50 MeV/u. Data are represented by dots. QT (dashed line), MRS (dotted line) and total (full line) contributions are shown. Statistical uncertainty is illustrated.

1. Proton multiplicities are significantly higher for the ^{58}Ni QP than the neutron multiplicities for the ^{58}Ni QT. This enhancement of free protons can be partially understood if we assume a rather symmetric (N/Z=1.07) nucleus that deexcites to reach the more neutron-rich evaporation attractor line [26] and thus emits more protons than neutrons. However, the observed quantitative difference cannot be fully explained by this scenario and other effects occuring in the dynamical deformation (neck) step of the collision should also contribute to this difference by lowering the N/Z ratio of the QP before its deexcitation begins (see section 4). Neutron multiplicities deduced for the target and the MRS in the system ^{36}Ar+^{58}Ni are used to evaluate the neutron multiplicities for the QP and the MRS in the symmetric ^{58}Ni+^{58}Ni reaction. In order to compare the two experiments, it is assumed that if the ^{58}Ni QP in the ^{58}Ni+^{58}Ni reaction and the ^{58}Ni QT in the ^{36}Ar+^{58}Ni reaction have the same excitation energy per nucleon, they will emit the same number of free neutrons. Excitation energy evaluation is achieved with the relation:

$$(\frac{E^*}{A})_{QP} = C(\frac{Z_{proj}-Z_{res}}{Z_{proj}}) \quad (3)$$

where C is assumed to be the same constant for both ^{36}Ar and ^{58}Ni. This assumption was verified by evaluating eq.(3) for the QP excitation

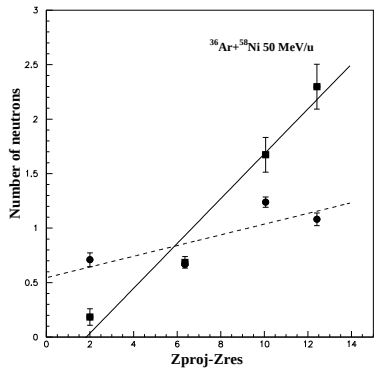

FIG. 3: Linearized neutrons multiplicities for ^{36}Ar+^{58}Ni at 50 MeV/u as a function of the projectile charge minus the QP residue charge. QT (dots) and MRS (squares) multiplicities are illustrated.

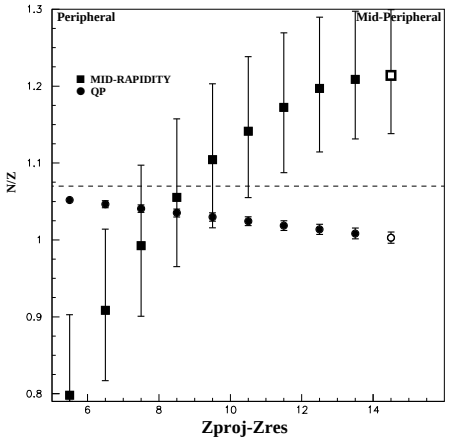

FIG. 4: N/Z of QP and MRS for the reaction ^{58}Ni+^{58}Ni at 52 MeV/u as a function of the charge difference between the projectile and the residue. Full squares: N/Z of MRS, full dots: N/Z of QP , thin dotted line: original N/Z of the projectile and target (1.07). Open symbols: extrapolation of results using Z_{res}(^{36}Ar)=4 for Z_{res}(^{36}Ar)=3.5. Errors due to multisource fit uncertainty for free nucleons are reported.

energy (calorimetry method) in the ^{58}Ni+^{58}Ni reaction and comparing it with calorimetry results for ^{40}Ar in Ref.[30].

Since HERACLES gives the charge of the ^{36}Ar projectile residue and not the charge of the ^{58}Ni target residue, two limiting assumptions were made to deduce the excitation energy of the ^{58}Ni QT, related to the charge of the target residue by eq.(3): equal energy sharing (EES) and another one approching the equal temperature limit (ETL). In the EES case, the total excitation energy available is split equally between the two partners regardless of their mass, in contrary to the ETL hypothesis in which a temperature equilibration (same E*/A for both partners) is supposed. Results of energy sharing experiments at intermediate energy show a clear tendency toward the EES hypothesis for a large range of centralities [31]. Since both hypotheses were found to give the same physics trends and to bring the same conclusion, for simplicity, only the results concerning the EES hypothesis will be presented. For each event analyzed in the ^{58}Ni+^{58}Ni reaction, the charge of the ^{58}Ni QP residue is taken as the charge of the ^{58}Ni QT residue in the ^{36}Ar+^{58}Ni reaction. Then a neutron multiplicity is selected according to the linearized relation of Fig. 3 and the EES hypothesis. Neutron multiplicities for the MRS have been added in the ^{58}Ni+^{58}Ni analysis according to the same excitation energy deduced for the QP. However, since those neutron multiplicities were extracted in the ^{36}Ar+^{58}Ni reaction, they should represent a lower limit for the heavier and more neutron-rich system ^{58}Ni+^{58}Ni.

4. N/Z VALUES FOR MRS AND QP

On an event-by-event basis, the ^{58}Ni QP and the MRS were reconstructed and free nucleon multiplicities were added according to the moving source parameter values for corresponding Z_{res}(^{58}Ni). Linearized multiplicity relations of Fig. 1 and Fig. 3 are used. Total N/Z composition for the total MRS and QP nuclear material (free nucleons, particles and all heavier fragments) as a function of Z_{proj}-Z_{res} is presented in Fig. 4. The general trend is that the N/Z ratio of the QP decreases sligthly with the centrality of the collision while the N/Z of the MRS increases for more central collisions, to reach a higher N/Z value than that of the QP and that of the original system (1.07). On average, the QP (and presumably the QT) seems to transfer a small number of neutrons to the MRS, that does not affect much its numerical N/Z value due to its larger size. However, this small amount of neutrons does enhance the neutron richness of the MRS due

to its smaller size. According to the QP and MRS N/Z ratios in Fig. 4, that neutron transfer is seen to increase with centrality, meaning that it could depend on the contact time of the two nuclei and on the deformation between them. For the most central collisions, MRS N/Z ratio reaches values of 1.2. For the same reaction, the QP N/Z drops at values close to 1. In an equal-mass reaction like ^{58}Ni+^{58}Ni, symmetry can be assumed in the dynamical deformation between target and projectile [14] so that QP and QT should, on average, have an equal contribution to the population of the MRS. This leads to believe that the N/Z results in Fig. 4 for the most peripheral reactions are non-physical. Indeed, the fact that both MRS and QP present a N/Z ratio below 1.07 simultaneously is impossible if the measurement of the QP and MRS is complete. Further analysis and BUU simulations show that there are neutrons missing in the reconstruction of the ^{58}Ni+^{58}Ni MRS and that the non-physical part of Fig. 4 could be due mainly to this. According to those results to be published, the numerical value of the MRS N/Z ratio would also be higher than in Fig. 4.

A possible schematic explanation to the results obtained here is that the projectile and target lose nuclear material in the midrapidity region during the time of contact between them and that there is a net flow of neutrons in the MRS during this phase of the reaction leaving the QP and QT neutron-poor in comparaison to their initial N/Z value. This fact would explain the low number of free neutrons, compared to free protons, emitted subsequently by the QP to reach the attractor line.

5. CONCLUSION

In summary, we observed that there is a neutron enrichment of the MRS in the reaction ^{58}Ni+^{58}Ni at 52 MeV/u. This was done by applying a statistical QP reconstruction procedure, using isotopically resolved fragments up to Z=4 in the INDRA multidetector, assumptions on the mass of the heavier fragments using evaporation model [26], and an estimate of free nucleon multiplicities deduced via a moving source analysis in the reactions ^{58}Ni+^{58}Ni at 52 MeV/u and ^{36}Ar+^{58}Ni at 50 MeV/u. The MRS N/Z ratio reaches a value higher than that of the initial system (1.07) and higher than that of the QP which decreases slightly to a value less than the initial system.

[1] J. Toke et al., Phys. Rev. Lett. **75**, 2920(1995).
[2] J. Lukasik et al. INDRA col., Phys. Rev. **C 55**, 1906(1997).
[3] C.P. Montoya et al., Phys. Rev. Lett. **73**, 3070(1994).
[4] J.F. Lecolley et al., Phys. Lett.B **354**, 202(1995).
[5] Y. Larochelle et al., Phys. Rev. **C 55**, 1869(1997).
[6] T. Lefort et al., Nucl. Phys. **A662**, 397(2000).
[7] L. Gingras et al., Phys. Rev. **C 65**, 061604(2002).
[8] S. Piantelli et al., Phys. Rev. Lett. **88**, 052701(2002).
[9] Z. He et al., Phys. Rev. **C 65**, 014606(2002).
[10] G. Poggi., Nucl. Phys. **A685**, 296(2001).
[11] D. Doré., Phys. Lett.B **491**, 15(2000).
[12] J. Colin et al., Phys. Rev. **C 67**, 064603(2003).
[13] Ph. Eudes et al., Phys. Rev. **C 56**, 2003(1997).
[14] A. Chernomoretz et al., Phys. Rev. **C 65**, 054613(2002).
[15] Y. Larochelle et al., Phys. Rev. **C 62**, 051 602(R)(2000).
[16] J. F. Dempsey et al., Phys. Rev. **C 54**, 1710(1996).
[17] E. Plagnol et al., Phys. Rev. **C 61**, 014 606(1999).
[18] P.M. Milazzo et al., Phys. Lett.B **509**, 204(2001).
[19] L.G. Sobotka et al., Phys. Rev. **C 62**, 031 603(R)(2000).
[20] A.S. Botvina and I.N. Mishustin., Phys. Rev.**C 63**, 061601(2001).
[21] H. Müller and B.D. Serot., Phys. Rev. **C 52**, 2072(1995).
[22] M. di Toro et al., Nucl. Phys. **A681**, 426c(2001).
[23] V. Baran et al., Nucl. Phys. **A632** , 287(1998).
[24] J. Pouthas et al., Nucl. Inst. and Meth. **A357**, 418(1995).
[25] N. Nakao et al., NIM **A362**, 454(1995).
[26] R. J. Charity., Phys. Rev. **C 58**, 1073(1998).
[27] L. Gingras et al., XXXVI International Winter Meeting On Nuclear Physics, Bormio (Italy), 265(1998).
[28] R. Wada et al., Phys. Rev. **C 39**, 497(1989).
[29] Y. Larochelle et al., Phys. Rev. **C 59**, 565(1999).
[30] G. Lanzano et al., Nucl. Phys. **A683**, 566(2001).
[31] G. Casini et al., Eur. Phys. **J A9**, 491(2000).